

Manipulating intertwined orders in solids with quantum light

Jiajun Li and Martin Eckstein

Institute of Theoretical Physics, University of Erlangen-Nuremberg, 91052 Erlangen, Germany

(Dated: August 4, 2022)

Intertwined orders exist ubiquitously in strongly correlated electronic systems and lead to intriguing phenomena in quantum materials. In this paper, we explore the unique opportunity of manipulating intertwined orders through entangling electronic states with quantum light. Using a quantum Floquet formalism to study the cavity-mediated interaction, we show the vacuum fluctuations effectively enhance the charge-density-wave correlation, giving rise to a phase with entangled electronic order and photon coherence, with putative superradiant behaviors in the thermodynamic limit. Furthermore, upon injecting even one single photon in the cavity, different orders, including s -wave and η -paired superconductivity, can be selectively enhanced. Our study suggests a new and generalisable pathway to control intertwined orders and create light-matter entanglement in quantum materials. The mechanism and methodology can be readily generalised to more complicated scenarios.

Introduction. The understanding and control of intertwined orders in strongly correlated materials and heterostructures are central issues in modern condensed matter physics [1–6]. Floquet engineering is one of the most promising pathways to effectively control intertwined orders in non-equilibrium [7–10]. By driving with strong laser pulses, intriguing scenarios have been implemented in quantum materials, such as apparent light-induced superconductivity and an anomalous quantum Hall effect [11–13]. Recently, an alternative pathway to implement strong light-matter coupling has attracted intense research interests. By coupling the system with an optical cavity [14, 15], the material is placed in an electromagnetic environment similar to a laser-driven system, holding the promise of engineering material properties without generating excess heating [16–25].

Of particular interest are systems where competing phases can be controlled via the quantum field. Beyond the aspect of material control, strong light-matter coupling in such a situation may lead to exotic hybrid phases in which quantum states of different macroscopic nature are entangled with the vacuum or single photons, similar to experiments which have demonstrated entanglement between clouds of individual emitters via photon exchange [26]. A paradigmatic example is the competition of charge-density wave (CDW) and superconducting (SC) phases for attractive electron-electron interactions, as minimally described by the attractive Hubbard model [27]. Classical Floquet engineering lifts the degeneracy between CDW and SC phases, and provides pathways to control the two phases separately [28, 29]. As there is a clear analogy between Floquet engineering and quantum electrodynamics [30, 31], one may speculate a similar controllability of the competing phases in the attractive Hubbard model via quantum light.

In spite of its similarity to Floquet engineering, the coupling to vacuum fluctuations does not automatically allow for the same degree of control over the material properties. For example, the coupling to vacuum fluctuations

in the repulsive Hubbard model cannot reverse the sign of exchange interactions [32], as possible with Floquet engineering [33]. It is therefore interesting to analyze the hybrid light-matter states both in the ground state and the excited states of the cavity. A systematic theory of the cavity-coupled solids for such excited or driven cavity states is still at its infancy. In particular, the gauge-invariant light-matter coupling is highly non-linear, and a naive truncation can lead to unphysical results [21, 34, 35]. In this paper, we use a quantum Floquet formalism to examine the possibility of controlling competing phases by creating highly entangled electronic and photon states in quantum materials. We show that the ground state of the cavity-coupled attractive Hubbard mode features entangled electronic order and photon coherence, with an enhancement of the charge density wave (CDW) order. With appropriate protocols, it is possible to selectively enhance CDW, s -wave and even η -pairing superconductivity (SC) [36] by creating more photons in the cavity. The conclusions are confirmed with the exact diagonalization of 1D Hubbard chains.

Quantum Floquet formalism. We consider a half-filled attractive Hubbard model coupled to a photon mode with polarization \mathbf{e}_p . For simplicity we consider the 1D case, with \mathbf{e}_p parallel to the chain. (The formalism presented below is independent of dimensionality.) The Hamiltonian reads

$$\hat{H} = -t_0 \sum_{\langle ij \rangle \sigma} e^{i\hat{\phi}_{ij}} c_{i\sigma}^\dagger c_{j\sigma} - U \sum_i n_{i\uparrow} n_{i\downarrow} + \Omega a^\dagger a, \quad (1)$$

where $\hat{\phi}_{ij} = \mathbf{A} \cdot \mathbf{d}_{ij} = g \xi_{ij} (a + a^\dagger)$ is the Peierls phase with bond dipole \mathbf{d}_{ij} and vector potential $\mathbf{A} = \mathbf{e}_p A_0 (a + a^\dagger)$, i.e., $\xi_{ij} = 1$ for hopping parallel to the polarization and is -1 for the anti-parallel direction, and $g = |\mathbf{d}_{ij}| A_0$ is the dimensionless coupling parameter. The corresponding electric field is, as usual, $\mathbf{E} = i \mathbf{e}_p \Omega A_0 (a - a^\dagger)$. Note that the above Hamiltonian is explicitly gauge-invariant and retains all the higher-order coupling terms, including the so-called diamagnetic term (\mathbf{A}^2) [21].

For $g = 0$, the model features degenerate ground states of CDW and s -wave SC order, due to the $SO(4)$ symmetry. The fate of the intertwined CDW and SC orders is altered by the *cavity-mediated interaction*, which is studied in a Floquet-like formalism below. The latter is similar in spirit as some recent works [30–32], but will be formulated more explicitly in a photon-number basis. We expand the Hamiltonian (2) in the photon number basis $\hat{H} = \sum_{nm} (\mathbb{I}_{el} \otimes |n\rangle \langle n|) \hat{H} (\mathbb{I}_{el} \otimes |m\rangle \langle m|) = \mathcal{H}_{nm} \otimes |n\rangle \langle m|$, where \mathbb{I}_{el} is the identity operator in the electronic Hilbert space, and introduce the *quantum* Floquet matrix

$$\mathcal{H}_{nm} = \mathcal{H}_{nm}^0 - (U \sum_i n_{i\uparrow} n_{i\downarrow} + n\Omega) \delta_{nm}$$

$$\text{with } \mathcal{H}_{nm}^0 = t_0 \sum_{\langle ij \rangle \sigma} i^{|n-m|} \xi_{ij}^{n-m} j_{n,m} c_{i\sigma}^\dagger c_{j\sigma}, \quad (2)$$

where $\langle n | e^{i\hat{\phi}_{ij}} | m \rangle = i^{|n-m|} \xi_{ij}^{n-m} j_{n,m}$ represent the matrix elements of the Peierls phase. They can be evaluated as a *finite* sum [37],

$$j_{n,m} = e^{-g^2/2} \sum_{k=0}^m \frac{(-1)^k g^{2k+|n-m|}}{k!(k+|n-m|)!} \sqrt{\frac{n!}{m!}} \frac{m!}{(m-k)!}, \quad (3)$$

for $n > m$ and $j_{n,m} = j_{m,n}$. The expression for \mathcal{H}_{nm} resembles the Floquet matrix Hamiltonian [38], but unlike the latter it is not translationally invariant in the photon index ($\mathcal{H}_{nm}^0 \neq \mathcal{H}_{n+\ell, m+\ell}^0$), and the indices are restricted to $n, m \geq 0$. Nevertheless, in the semi-classical limit $n, m \rightarrow \infty$ with $g\sqrt{n}$ finite [31], $j_{n,m}$ converges to the Bessel function $J_{|n-m|}(2g\sqrt{n})$, so that Eq. (2) recovers the Floquet Hamiltonian (appendix). Moreover, similar to the Bessel functions, the function $j_{n,m}$ decay super-exponentially as $|n-m| \rightarrow \infty$, which decouples the quantum Floquet bands for large $|n-m|$ and allows for efficient numerical evaluations.

Strong coupling expansion. The quantum Floquet Hamiltonian, similar to the classical Floquet approach, provides an intuitive picture of the underlying physics. For example, the hopping of an electron can result in a shift of the quantum Floquet index n , corresponding to the emission or absorption of photons. Technically, this allows for a systematic strong coupling expansion. Assuming off-resonance $\Omega \neq U$, the low-energy physics of (2) in the limit $U \gg t$ can be captured by an effective pseudospin model [27, 28] from a Schrieffer-Wolff transformation. When projected to a given photon number sector n , the effective Hamiltonian reads $H_{nn}^{\text{eff}} = \sum_l \mathcal{P}_0 \mathcal{H}_{n, n+l}^0 \mathcal{P}_1 \mathcal{H}_{n+l, n}^0 \mathcal{P}_0 / (U + l\Omega)$, where \mathcal{P}_i is the projection operator to the subspace of i electronic excitations. One obtains

$$H_{nn}^{\text{eff}} = \frac{1}{2} J_{\text{ex}}^{SC} \sum_{\langle ij \rangle} (\eta_i^+ \eta_j^- + \text{h.c.}) + J_{\text{ex}}^{CDW} \sum_{\langle ij \rangle} \eta_i^z \eta_j^z, \quad (4)$$

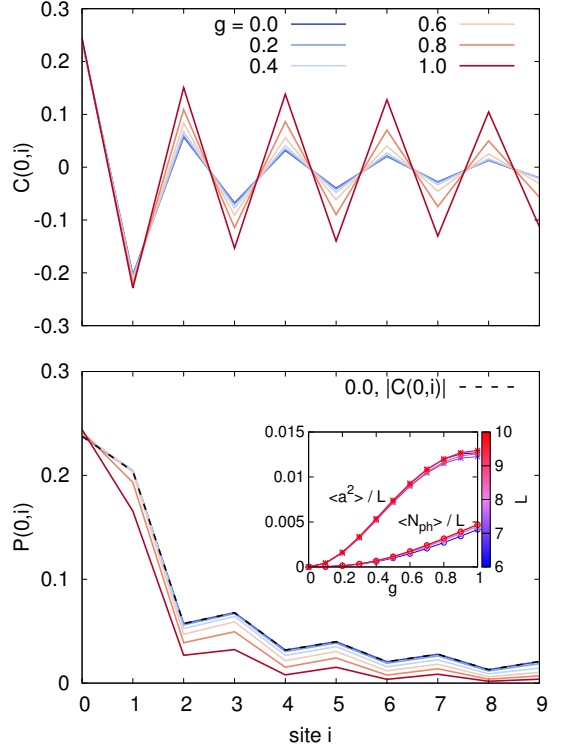


FIG. 1. Spatial correlation of charge ($C(0, i)$) and superconducting ($P(0, i)$) order for increasing photon coupling g , for $U = 8.0t_0$ and $\Omega = 6.0t_0$. The dashed line in the lower panel shows the absolute value $|C(0, i)|$ at $g = 0$ for comparison. The inset shows the photon occupation $N_{ph} = \langle a^\dagger a \rangle$ and $\langle a^2 \rangle$, scaled with $L = 6, \dots, 10$.

where the η -pseudospin is defined as

$$\eta_i^+ = (\eta_i^-)^\dagger = (-1)^i c_i^\dagger c_j^\dagger,$$

$$\eta_i^z = (n_i - 1)/2, \quad (5)$$

so η^\pm represents pairing and η^z corresponds to charge. In the uncoupled ($g = 0$) case $J_{\text{ex}}^{SC} = J_{\text{ex}}^{CDW} = J_{\text{ex}} = 2t_0^2/U$. For $g \neq 0$, the exchange coupling contains contributions from all virtual hopping processes with intermediate states in different photon-number sectors (labeled by l) and the processes associated with J^{SC} and J^{CDW} capture different phase factors [28],

$$\left\{ \begin{array}{c} J_{\text{ex}}^{SC} \\ J_{\text{ex}}^{CDW} \end{array} \right\} = J_{\text{ex}} \sum_{l \geq -n}^{\infty} \left\{ \begin{array}{c} (-1)^l \\ +1 \end{array} \right\} \frac{j_{n, n+l} j_{n+l, n}}{1 + l\Omega/U}. \quad (6)$$

The full strong-coupling model also contains a pseudospin-photon coupling which is off-diagonal in the photon number (see below), but for $\Omega \gg J_{\text{ex}}$, transitions between photon sectors are suppressed and the electronic configuration is determined by Eq. (4) for fixed n .

Entangling orders with vacuum fluctuations. In the cavity ground state ($n = 0$) the induced interaction exclusively enhances J^{CDW} and suppresses J^{SC} irrespective of the values of U and Ω , because $j_{i,0} =$

$e^{-g^2/2}g^l/\sqrt{l!} > 0$. The relevant factor $e^{-g^2/2}$ is due to the cavity-induced dynamical localization [31]. This behavior is dramatically different from classical Floquet driving, where a blue-detuned light ($\Omega > U$) enhances superconductivity [28, 29, 39]. To confirm this prediction from the effective pseudospin model, we solve the original Hamiltonian (1) using exact diagonalization (ED). The ground state is obtained with the Lanczos algorithm, assuming half-filling and $\hat{S}_z = 0$. Fig. 1 shows the charge and pairing correlation functions $C(0, i) = \langle \eta_0^z \eta_i^z \rangle$ and $P(0, i) = \frac{1}{2} \langle \eta_0^+ \eta_i^- \rangle$ for a chain of $L = 10$ with open boundary condition. At $g = 0$, both functions have identical magnitude. As g increases, a staggered CDW correlation is continuously enhanced, while SC is suppressed. The same qualitative behavior is observed for $\Omega > U$, although the effect is weaker due to a larger denominator $1/(U + l\Omega)$ in Eq. (6). This confirms our analytic theory.

Another intriguing aspect is the emergent light-matter mixing. Indeed, the photon occupation $N_{ph} = \langle a^\dagger a \rangle$ scales almost linearly with system size L (Fig. 1 inset), implying a macroscopic $\langle a^\dagger a \rangle \sim L$ in the thermodynamic limit, or a superradiant phase [40]. In the strong coupling picture, the light-matter entangling comes from two facts: (i) In the Schrieffer-Wolff transformation, photon operators are dressed, and the photon number n in Eq. (4) differs from the bare $\langle a^\dagger a \rangle$. The non-zero $\langle a^2 \rangle$ shows that the dressed zero-photon state has some squeezed character (though $\langle a \rangle = 0$). (ii) Moreover, when we restore the photon operators in the Hamiltonian [31], up to first order in g one gets a (somewhat expected) Dicke-type coupling $g_{\text{eff}} i(a - a^\dagger) \sum_{\langle ij \rangle} \xi_{ij}(n_i - n_j)$, where g_{eff} is of order gt_0^2/U . For an open chain the total charge polarization $P = n_0 - n_{L-1}$ therefore couples to the electric field $ig(a - a^\dagger)$ [29, 41]. CDW configurations with $P > 0$ ($n_0 = 2, n_{L-1} = 0$ in the extreme case) and $P < 0$ thus entangle with the photon states of $\langle \mathbf{E} \rangle \propto \pm \mathbf{e}_p$, which explains the behavior observed in Fig. 2.

The light matter entangling motivates us to highlight an intriguing consequence: after a projective measurement of the field amplitude (with projection $\Pi_A = |iA\rangle \langle iA|$ on a coherent state), the matter is left in states of different charge polarization P (Fig. 2). The light-matter coupling obviously displaces the coherent amplitude and induces two symmetric peaks $A \sim \pm 1$ (see panel (a)), corresponding to two degenerate CDW states of opposite charge polarization P . While the global system does not break the symmetry, the light-matter wave function has its weight centered at contributions which separately break the symmetry in the matter, and are aligned with a corresponding field configuration [42].

Enhanced SC in the few-photon regime. To explore the possibility of selectively enhancing different orders, we now turn to the case of a driven cavity. Physically, we address this regime by injecting a finite number n of photons into the cavity. The key difference between $n = 0$ and $n > 0$ in the couplings Eq. (6) is the existence

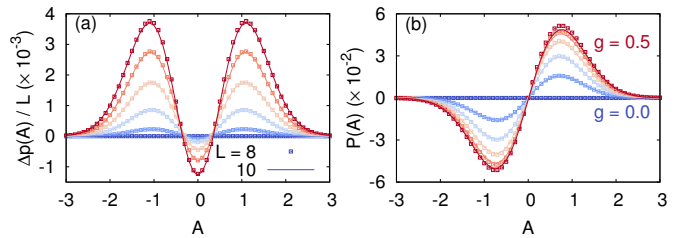


FIG. 2. Entanglement of the electronic order and photon coherent states. (a) Difference of probability $p(A) = \text{Tr}(\rho_G \Pi_A)$ for varying g and the uncoupled case ($g = 0$). $\rho_G = |GS\rangle \langle GS|$ is the ground state density matrix. The values are normalized by $1/L$. (b) Charge polarization when measured in the projected state, i.e. $P(A) = \text{Tr}[(n_0 - n_{L-1})\rho_G \Pi_A]$. Colors from blue to red indicate coupling $g = 0.0, 0.1, \dots, 0.5$.

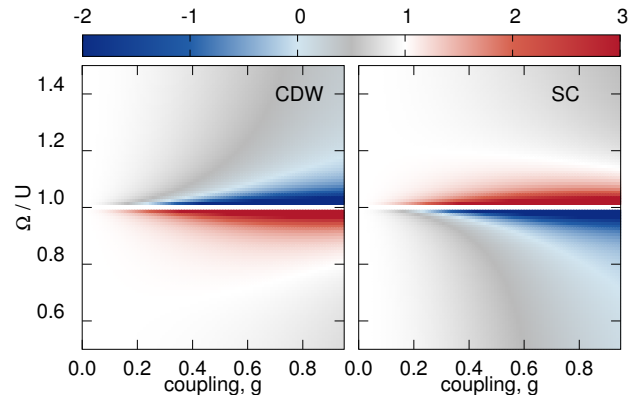


FIG. 3. The selective enhancement of different orders in the presence of one photon. The color represents the value of J_{ex}^{SC} and J_{ex}^{CDW} normalized by the uncoupled $J_{\text{ex}}(0) = 2t_0^2/U$. The exchange coupling is enhanced in the red region and suppressed in the grey region. In particular, the exchange coupling changes its sign in the blue region.

of intermediate states with $l < 0$ (photon absorption), which contribute *negative* denominators $1 + l\Omega/U$. Even the presence of a single photon allows the selective enhancement of CDW and SC orders, see Fig. 3. In general, the CDW is enhanced in the red-detuned regime, while the SC is enhanced in the blue-detuned regime. More interestingly, there is a wide regime (though being close to the resonance $\Omega \sim U$) where the exchange coupling changes its sign. In this case, a negative J_{ex}^{SC} favors the staggered, or η -paired superconductivity [28, 43, 44], and a negative J_{ex}^{CDW} leads to a trend of *charge segregation*, where doublons tend to stick together and repel holons. The same qualitative physics is found for more photons $N_{ph} \geq 2$.

In a real experiment, the multi-photon regime is realized through driving with an external laser field, which does not necessarily lead to a Fock state. However, the fine control of cavity photon number is supported by the strong non-linear effects of light-matter coupling. Specif-

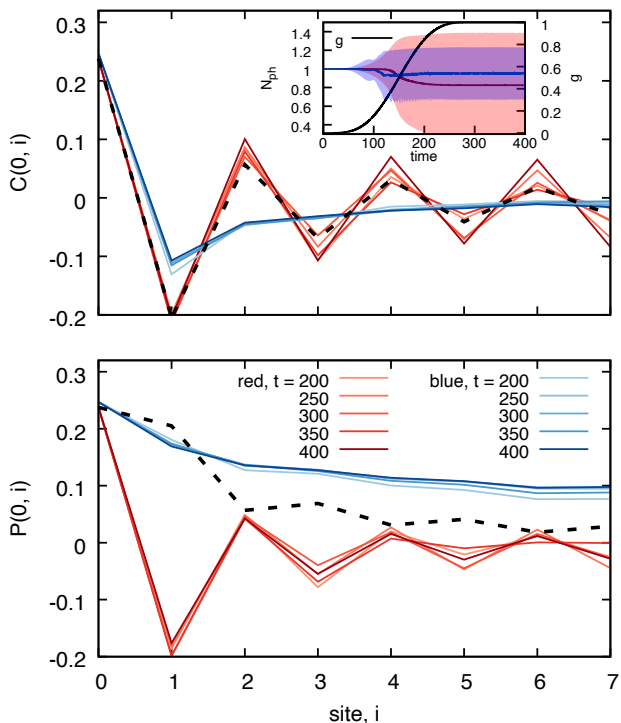


FIG. 4. The evolution of charge and pairing correlations under the injection of one photon. The red curves represent the red-detuned case $\Omega = 0.5U$ while the blue curves represent the blue-detuned case $\Omega = 1.5U$. The dashed line represents the initial state $g = 0.0$ (ground state without light-matter coupling). The inset shows the quench profile of coupling g from 0.0 to 1.0 and the evolution of photon number in the cavity. The shaded area covers the region of $N_{ph}(t) \pm \Delta N_{ph}(t)$ where $\Delta N_{ph} = \langle a^\dagger a a^\dagger a \rangle - \langle a^\dagger a \rangle^2$ is the uncertainty of photon number.

ically, the injection of one photon into the cavity modifies the “internal state” of the cavity-matter system, changing the energy cost of injecting a second photon (appendix). The external driving can, therefore, be made resonant with selected photon numbers.

To numerically study the few-photon regime, we start with the uncoupled case ($g = 0$) and prepare the matter in its ground state and the cavity in a photon-number state ($|n = N_{ph}\rangle$). The coupling g is then turned on *adiabatically*. When the resulting state is protected by a gap, the adiabatic theorem guarantees that it is the lowest-lying state within the subspace $n = N_{ph}$. In general, the final state can mix with other photon-number sectors and should approximate the *in-state* of the corresponding quantum scattering problem. We solve the time-evolution of the cavity-coupled Hubbard chain of $L = 8$ using a Krylov-space algorithm for iteration number 80. The coupling g is raised to a very large value $g = 1.0$ for demonstration.

The result is shown in Fig. 4. As g is turned on, the photon number drops from $N_{ph} = 1$ to 0.953 for $\Omega = 1.5U$ (blue-detuned) and to 0.826 for $\Omega = 0.5U$ (red-

detuned). In contrast to the ground state, the CDW becomes significantly suppressed while the SC is enhanced for the blue-detuned cavity. Thus, an entangled photon-order state distinct from the equilibrium is dynamically created by driving. In the red-detuned case the CDW order is again enhanced, but, instead of a strong suppression, the pairing correlation is turned into a staggered form, i.e., the η -pairing SC. Although the η -pairing is expected in some parameter regime due to the sign reversal of J_{ex}^{SC} , the exchange coupling is predicted to be almost zero in the calculated case. Instead, the production of η -pairing should be attributed to the photon absorption (see the inset of Fig. 4), which pumps up η -paired states due to a selection rule imposed by the $SO(4)$ symmetry [45, 46].

Remarks on the BCS limit. So far we have concentrated on the strong coupling or BEC limit [27], where projecting out higher excited states is justified. One can nevertheless integrate out the photon mode without projecting to the sector of zero electronic excitation in the limit $\Omega \gg t_0$, which results in the simplified $H_{nn}^{\text{eff}} = \mathcal{H}_{nn} + \sum_l \mathcal{H}_{n,n+l}^0 \mathcal{H}_{n+l,n}^0 / \Omega$. In particular, this induces a next-to-nearest-neighbor (NNN) hopping and a two-site interaction $I_1(\eta_i^\dagger \eta_j^- + \text{h.c.}) + 2I_2 \eta_i^z \eta_j^z + 2I_2 \mathbf{S}_i \cdot \mathbf{S}_j$, with coefficients $I_1 = \sum_{l > -n, l \neq 0} j_{n,n+l} j_{n+l,n} / \Omega$ and $I_2 = \sum_{l > -n, l \neq 0} (-1)^l j_{n,n+l} j_{n+l,n} / \Omega$, leading to qualitatively similar physics as described in the BEC limit. Note that the cavity also induces a long-range interaction close to the ground state, which is, for the lowest order, of current-current type [18]. This may complicate the scenario in certain parameter regimes. A systematic examination in this regime as well as the BCS-BEC crossover is reserved for the future.

Conclusion. The coupling to an optical cavity provides a powerful toolbox to simultaneously manipulate intertwined orders in solids and engineer the cavity photon mode. In this paper, we demonstrate the concept using a minimal model of competing CDW and SC orders, the cavity-coupled attractive Hubbard model, solved by an analytic theory based on the quantum Floquet formalism, and then confirmed by exact diagonalization for 1D chains. It turns out the vacuum fluctuations become entangled with the electronic ordering and enhance exclusively the CDW order, giving rise to a putative superradiant condensate for large system sizes. This differs dramatically from the Floquet-engineering scenarios. By injecting few photons in the cavity, one can furthermore selectively enhance different orders, including CDW, s -wave SC, and η -pairing SC in different parameter regimes.

The manipulation of intertwined orders originates from a renormalization of the short-range exchange interaction, and can be detectable in some transition metal compounds, e.g., cuprates and iridates [47, 48]. Fermionic cold atom systems are promising candidates for showing the photon-order entanglement [49]. The quantum Flo-

quet formalism provides a natural framework to unify the quantum driving and the classical Floquet scenarios [50], and can be combined with established numerical methods, such as dynamical mean-field theory and its extensions [38, 51, 52] to describe more complicated systems [53, 54]. We have concentrated on the adiabatic driving regime, while non-adiabatic processes can enhance the dynamical generation of entanglement, opening up further chances of quantum light engineering. To study these effects, a full description of the dissipative cavity is necessary [23, 55].

We thank M. A. Sentef for useful discussions. This work was supported by ERC Starting Grant No. 716648.

-
- [1] S. A. Kivelson, I. P. Bindloss, E. Fradkin, V. Oganessian, J. M. Tranquada, A. Kapitulnik, and C. Howald, *Rev. Mod. Phys.* **75**, 1201 (2003).
- [2] G. Ghiringhelli, M. Le Tacon, M. Minola, S. Blanco-Canosa, C. Mazzoli, N. B. Brookes, G. M. De Luca, A. Frano, D. G. Hawthorn, F. He, T. Loew, M. M. Sala, D. C. Peets, M. Salluzzo, E. Schierle, R. Sutarto, G. A. Sawatzky, E. Weschke, B. Keimer, and L. Braicovich, *Science* **337**, 821 (2012), <https://science.sciencemag.org/content/337/6096/821.full.pdf>
- [3] J. Chang, E. Blackburn, A. Holmes, N. B. Christensen, J. Larsen, J. Mesot, R. Liang, D. Bonn, W. Hardy, A. Watenphul, *et al.*, *Nature Physics* **8**, 871 (2012).
- [4] J. M. Tranquada, B. J. Sternlieb, J. D. Axe, Y. Nakamura, and S. Uchida, *Nature* **375**, 561 (1995).
- [5] B. Sipos, A. F. Kusmartseva, A. Akrap, H. Berger, L. Forró, and E. Tutiš, *Nature materials* **7**, 960 (2008).
- [6] E. Fradkin, S. A. Kivelson, and J. M. Tranquada, *Rev. Mod. Phys.* **87**, 457 (2015).
- [7] D. N. Basov, R. D. Averitt, and D. Hsieh, *Nat. Mater.* **16**, 1077 (2017).
- [8] M. Bukov, L. D'Alessio, and A. Polkovnikov, *Advances in Physics* **64**, 139 (2015).
- [9] A. Eckardt, *Reviews of Modern Physics* **89**, 011004 (2017).
- [10] T. Oka and S. Kitamura, *Annual Review of Condensed Matter Physics* **10**, 387 (2019).
- [11] Y. Wang, H. Steinberg, P. Jarillo-Herrero, and N. Gedik, *Science* **342**, 453 (2013).
- [12] J. W. McIver, B. Schulte, F. U. Stein, T. Matsuyama, G. Jotzu, G. Meier, and A. Cavalleri, *Nature Physics* **16**, 38 (2020).
- [13] M. Buzzi, D. Nicoletti, M. Fechner, N. Tancogne-Dejean, M. A. Sentef, A. Georges, M. Dressel, A. Henderson, T. Siegrist, J. A. Schlueter, K. Miyagawa, K. Kanoda, M. S. Nam, A. Ardavan, J. Coulthard, J. Tindall, F. Schlawin, D. Jaksch, and A. Cavalleri, *arXiv e-prints*, arXiv:2001.05389 (2020), arXiv:2001.05389 [cond-mat.supr-con].
- [14] S. Smolka, W. Wuester, F. Haupt, S. Faelt, W. Wegscheider, and A. Imamoglu, *Science* **346**, 332 (2014), <https://science.sciencemag.org/content/346/6207/332.full.pdf>
- [15] A. Thomas, E. Devaux, K. Nagarajan, T. Chervy, M. Seidel, D. Hagenmüller, S. Schütz, J. Schachenmayer, C. Genet, G. Pupillo, *et al.*, *arXiv preprint arXiv:1911.01459* (2019).
- [16] M. A. Sentef, M. Ruggenthaler, and A. Rubio, *Science advances* **4**, eaau6969 (2018).
- [17] G. Mazza and A. Georges, *Physical review letters* **122**, 017401 (2019).
- [18] F. Schlawin, A. Cavalleri, and D. Jaksch, *Physical review letters* **122**, 133602 (2019).
- [19] F. Schlawin and D. Jaksch, *Physical review letters* **123**, 133601 (2019).
- [20] X. Wang, E. Ronca, and M. A. Sentef, *Phys. Rev. B* **99**, 235156 (2019).
- [21] J. Li, D. Golez, G. Mazza, A. Millis, A. Georges, and M. Eckstein, *arXiv preprint arXiv:2001.09726* (2020).
- [22] K. Lenk and M. Eckstein, *arXiv preprint arXiv:2002.12241* (2020).
- [23] H. Gao, F. Schlawin, A. Cavalleri, and D. Jaksch, *arXiv preprint arXiv:2003.05319* (2020).
- [24] Y. Ashida, A. Imamoglu, J. Faist, D. Jaksch, A. Cavalleri, and E. Demler, *arXiv e-prints*, arXiv:2003.13695 (2020), arXiv:2003.13695 [cond-mat.mes-hall].
- [25] J. Rohn, M. Hörmann, C. Genes, and K. P. Schmidt, *arXiv preprint arXiv:2003.05804* (2020).
- [26] B. Julsgaard, A. Kozhokin, and E. S. Polzik, *Nature* **413**, 400 (2001).
- [27] R. Micnas, J. Ranninger, and S. Robaszkiewicz, *Rev. Mod. Phys.* **62**, 113 (1990).
- [28] S. Kitamura and H. Aoki, *Physical Review B* **94**, 174503 (2016).
- [29] M. A. Sentef, A. Tokuno, A. Georges, and C. Kollath, *Physical review letters* **118**, 087002 (2017).
- [30] C. Schäfer, M. Ruggenthaler, and A. Rubio, *Physical Review A* **98**, 043801 (2018).
- [31] M. A. Sentef, J. Li, F. Künnzel, and M. Eckstein, *arXiv preprint arXiv:2002.12912* (2020).
- [32] M. Kiffner, J. R. Coulthard, F. Schlawin, A. Ardavan, and D. Jaksch, *Physical Review B* **99**, 085116 (2019).
- [33] J. Mentink, K. Balzer, and M. Eckstein, *Nature communications* **6**, 1 (2015).
- [34] M. Kiffner, J. R. Coulthard, F. Schlawin, A. Ardavan, and D. Jaksch, *Phys. Rev. B* **99**, 099907 (2019).
- [35] G. M. Andolina, F. M. D. Pellegrino, V. Giovannetti, A. H. MacDonald, and M. Polini, *Phys. Rev. B* **100**, 121109 (2019).
- [36] C. N. Yang and S. Zhang, *Modern Physics Letters B* **4**, 759 (1990).
- [37] See appendix.
- [38] N. Tsuji, T. Oka, and H. Aoki, *Physical Review B* **78**, 235124 (2008).
- [39] R. Fujiuchi, T. Kaneko, K. Sugimoto, S. Yunoki, and Y. Ohta, *arXiv preprint arXiv:2001.10708* (2020).
- [40] O. Viehmann, J. von Delft, and F. Marquardt, *Physical review letters* **107**, 113602 (2011).
- [41] S. Felicetti and A. Le Boité, *Phys. Rev. Lett.* **124**, 040404 (2020).
- [42] Note that in the language of macroscopic electrodynamics, $i(a - a^\dagger)$ is actually to the displacement field.
- [43] A. Rosch, D. Rasch, B. Binz, and M. Vojta, *Physical review letters* **101**, 265301 (2008).
- [44] J. Li, D. Golez, P. Werner, and M. Eckstein, *arXiv preprint arXiv:1908.08693* (2019).
- [45] T. Kaneko, T. Shirakawa, S. Sorella, and S. Yunoki, *Phys. Rev. Lett.* **122**, 077002 (2019).
- [46] T. Kaneko, S. Yunoki, and A. J. Millis, *arXiv e-prints*, arXiv:1910.11229 (2019), arXiv:1910.11229

[cond-mat.str-el].

- [47] B. Keimer, S. A. Kivelson, M. R. Norman, S. Uchida, and J. Zaanen, *Nature* **518**, 179 (2015).
- [48] I. Battisti, K. M. Bastiaans, V. Fedoseev, A. de la Torre, N. Iliopoulos, A. Tamai, E. C. Hunter, R. S. Perry, J. Zaanen, F. Baumberger, and M. P. Allan, *Nature Physics* **13**, 21 (2017).
- [49] A. Mazurenko, C. S. Chiu, G. Ji, M. F. Parsons, M. Kanász-Nagy, R. Schmidt, F. Grusdt, E. Demler, D. Greif, and M. Greiner, *Nature* **545**, 462 (2017).
- [50] T. Kitagawa, T. Oka, A. Brataas, L. Fu, and E. Demler, *Phys. Rev. B* **84**, 235108 (2011).
- [51] H. Aoki, N. Tsuji, M. Eckstein, M. Kollar, T. Oka, and P. Werner, *Reviews of Modern Physics* **86**, 779 (2014).
- [52] D. Golež, M. Eckstein, and P. Werner, *Phys. Rev. B* **100**, 235117 (2019).
- [53] J. B. Curtis, Z. M. Raines, A. A. Allocca, M. Hafezi, and V. M. Galitski, *Physical review letters* **122**, 167002 (2019).
- [54] M. Claassen, H.-C. Jiang, B. Moritz, and T. P. Devereaux, *Nature communications* **8**, 1 (2017).
- [55] D. Lentrodt and J. Evers, *Phys. Rev. X* **10**, 011008 (2020).

Appendix

The evaluation of quantum Floquet matrix Hamiltonian

In this section we show the evaluation of $\langle n | e^{i\hat{\phi}_{ij}} | m \rangle$. We use the Baker-Hausdorff formula $\exp(X + Y) = \exp(X) \exp(Y) \exp(-[X, Y]/2)$ when $[X, Y]$ is a c-number, then Taylor expand the exponential factor and reorder the sum,

$$\begin{aligned}
e^{i\xi_{ij}g(a+a^\dagger)} &= e^{i\xi_{ij}ga^\dagger} e^{i\xi_{ij}ga} e^{-g^2/2} \\
&= e^{-g^2/2} \sum_{kk'} \frac{(ig\xi_{ij}a^\dagger)^k (ig\xi_{ij}a)^{k'}}{k!k'!} \\
&= e^{-g^2/2} \left[\sum_k \frac{(-1)^k g^{2k}}{k!k!} (a^\dagger)^k a^k + \sum_{l>0} \sum_k \frac{(-1)^k g^{2k}}{k!(k+l)!} ((ig\xi_{ij})^l (a^\dagger)^{k+l} a^k + (ig\xi_{ij})^l (a^\dagger)^k a^{k+l}) \right] \\
&= \sum_l i^{|l|} \xi_{ij}^l \hat{\mathcal{J}}_l.
\end{aligned} \tag{7}$$

Here we have defined

$$\hat{\mathcal{J}}_l \equiv e^{-g^2/2} \sum_k \frac{(-1)^k g^{2k+|l|}}{k!(k+|l|)!} \begin{cases} (a^\dagger)^{k+|l|} a^k, & l \geq 0 \\ (a^\dagger)^k a^{k+|l|}, & l < 0 \end{cases}. \tag{8}$$

This functional satisfies $\hat{\mathcal{J}}_l^\dagger = \hat{\mathcal{J}}_{-l}$. We can, therefore, evaluate the quantum Floquet Hamiltonian and define $j_{n,m} = \langle n | \hat{\mathcal{J}}_{n-m} | m \rangle$. For $n > m$ one obtains

$$j_{n,m} = e^{-g^2/2} \sum_{k=0}^m \frac{(-1)^k g^{2k+|n-m|}}{k!(k+|n-m|)!} \sqrt{\frac{n!}{m!}} \frac{m!}{(m-k)!}, \tag{9}$$

and similarly for $n < m$

$$j_{n,m} = e^{-g^2/2} \sum_{k=0}^n \frac{(-1)^k g^{2k+|n-m|}}{k!(k+|n-m|)!} \sqrt{\frac{m!}{n!}} \frac{n!}{(n-k)!}. \tag{10}$$

The $j_{n,m}$ function is a finite sum which can readily be evaluated. As discussed in the main text, for $|n-m| \rightarrow \infty$, $j_{n,m}$ decays as $g^{|n-m|}/\sqrt{|n-m|!}$ so that the coupling between different quantum Floquet bands quickly decays to zero as $|n-m|$ increases.

The cavity to Floquet crossover in the semiclassical limit

In this section we explicitly show how the quantum Floquet Hamiltonian continuously converges to the Floquet Hamiltonian. This is essentially the crossover from quantum driving by fluctuations to semiclassical driving by a coherent classical field. We will follow the physical intuition of Ref. 31. Under periodic driving, where the *classical* vector potential $\mathcal{A} \cos \Omega t$ coupled through the Peierls phase $e^{i\xi_{ij}\mathcal{A} \cos \Omega t}$, the corresponding Floquet matrix Hamiltonian reads [38],

$$\mathcal{H}_{nm}^F = -t_0 \sum_{\langle ij \rangle \sigma} i^{|n-m|} \xi_{ij}^{n-m} J_{|n-m|}(\mathcal{A}) c_{i\sigma}^\dagger c_{j\sigma} + \left(U \sum_i n_{i\uparrow} n_{i\downarrow} + n\Omega \right) \delta_{nm}, \tag{11}$$

where $J_l(x)$ is the l th Bessel function of the first kind,

$$J_{|l|}(x) = \sum_k (-)^k \frac{(x/2)^{2k+|l|}}{k!(k+|l|)!}. \tag{12}$$

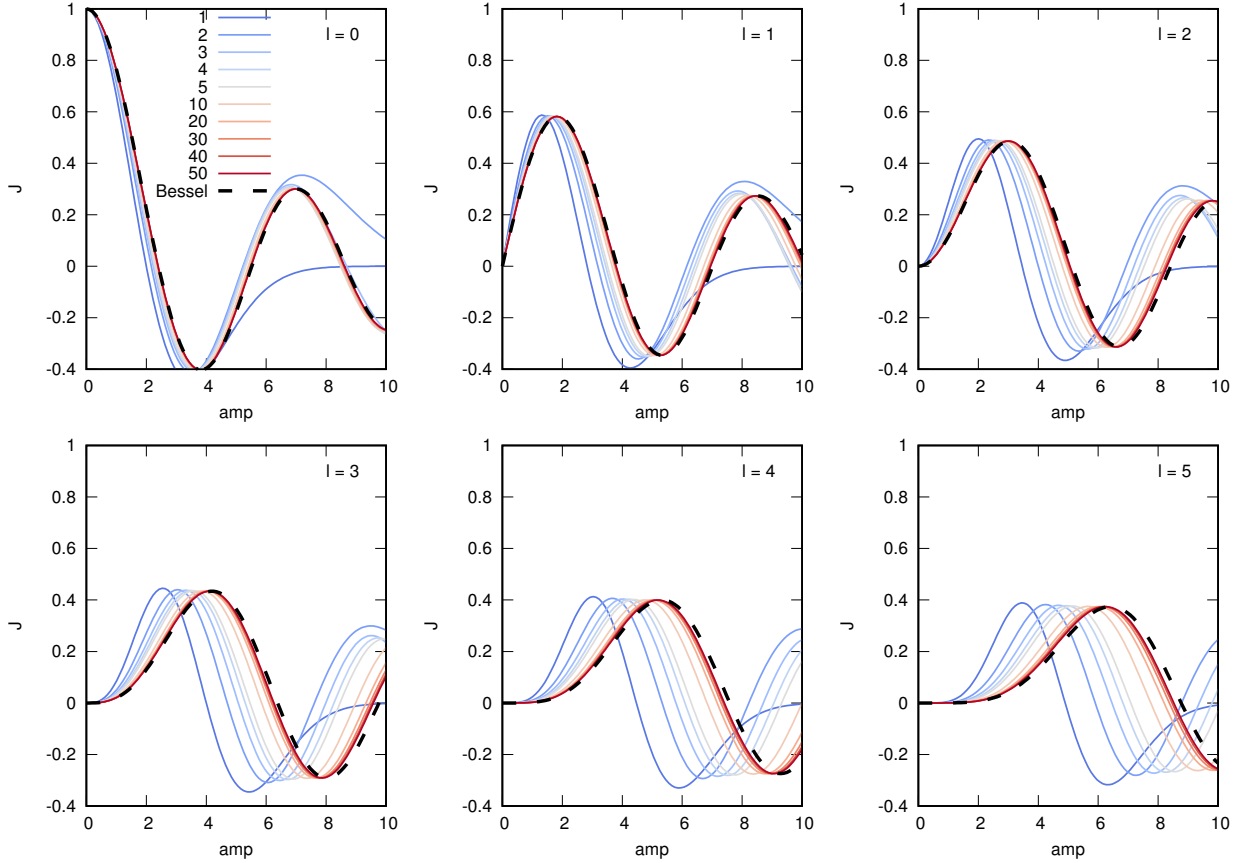


FIG. 5. The convergence of $j_{n,m}$ to the Bessel function $J_l(\mathcal{A})$ under the semiclassical limit. The amplitude is $\mathcal{A} = 2g\sqrt{n}$.

Back to our quantum Floquet formulation, in the semiclassical limit $n \rightarrow \infty$ and $g \rightarrow 0$, with $2g\sqrt{n} = \mathcal{A}$. Suppose $l \geq 0$, the $j_{n+l,n}$ function reads

$$\lim_{n \rightarrow \infty} j_{n+l,n} = \lim_{n \rightarrow \infty} e^{-\mathcal{A}^2/8n} \sum_{k=0}^n \frac{(-1)^k (|\mathcal{A}|/2)^{2k+|l|}}{k!(k+|l|)!} \sqrt{\frac{(n+|l|)!}{n!n^{|l|}}} \frac{n!}{(n-k)!n^k} = J_{|l|}(\mathcal{A}). \quad (13)$$

Note that $(n+|l|)!/n! \rightarrow n^{|l|}$ under the limit. This restores the Floquet-driven case where the vector potential $\mathbf{A} \cdot \mathbf{d}_{ij}$ is replaced by a Peierls phase $\xi_{ij}\mathcal{A} \cos(\Omega t)$. This limiting behavior is shown in Fig. 5. In the ground state the relevant photon-number sector is $n = 0$, the $j_{l,0}$ functions reduce to $j_{l,0} = e^{-g^2/2} g^l / \sqrt{l!}$, which are plotted in Fig. 6. For fixed g , $j_{l,0}$ simply gives the weight of the photon state $|l\rangle$ after the Peierls phase acting on the vacuum state, which leads to a coherent state, where $|j_{l,0}|^2$ is a Poisson distribution.

The light-matter coupling in the effective model

Under the strong-coupling expansion, the unperturbed electronic states $|s\rangle$'s (eigenstates of H_U) mix with different photon-number sectors according to the second-order perturbation theory in t_0/U . This introduces entanglement between electrons and the quantum light. Furthermore, when the CDW order is considered, one obtains further effective coupling between CDW and the electric field $\mathbf{E} = ig\Omega \mathbf{e}_p (a - a^\dagger)$.

As a heuristic method, we compute approximately the effective Hamiltonian at the strong U limit ($U \gg \Omega, t_0$). By

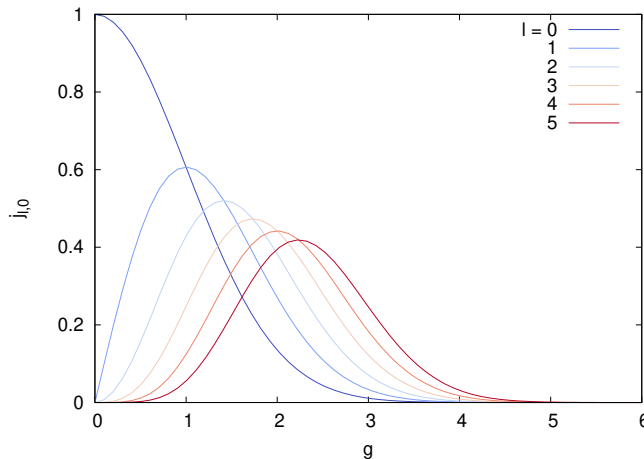


FIG. 6. The function $j_{l,0}(2|g|)$ for the dark cavity.

projecting out electronic excitations, the effective Hamiltonian within the n th photon-sector reads

$$\begin{aligned}
 H_{n+1,n}^{\text{eff}} &= \sum_m \mathcal{P}_0 \mathcal{H}_{n+1,m}^0 \mathcal{P}_1 \mathcal{H}_{m,n}^0 \mathcal{P}_0 / U \\
 &\approx \mathcal{P}_0 \mathcal{H}_{n+1,n}^0 \mathcal{P}_1 \mathcal{H}_{n,n}^0 \mathcal{P}_0 / U + \mathcal{P}_0 \mathcal{H}_{n+1,n+1}^0 \mathcal{P}_1 \mathcal{H}_{n+1,n}^0 \mathcal{P}_0 / U \\
 &\approx g \frac{2t_0^2}{U} i\sqrt{n+1} \sum_{\langle ij \rangle} \xi_{ij} (\eta_i^z - \eta_j^z)
 \end{aligned} \tag{14}$$

and similarly for $H_{n,n+1}^{\text{eff}}$. To restore the photon operators, we re-sum $H^{\text{eff}} \approx \sum_n (H_{n+1,n}^{\text{eff}} \otimes |n+1\rangle \langle n| + \text{h.c.})$ and identify $a^\dagger = \sum_n \sqrt{n+1} |n+1\rangle \langle n|$. Using the notation of (4), one then obtains a light-matter coupling term with the form $ig_{\text{eff}}(a - a^\dagger) \sum_{\langle ij \rangle} \xi_{ij} (\eta_i^z - \eta_j^z)$. Recall $\eta_i^z = (n_i - 1)/2$, the term turns out to be $ig_{\text{eff}}(a - a^\dagger)(n_0 - n_{L-1})$ for an open Hubbard chain of site number L . This term should be responsible for the double-peak structure shown in Fig. 2.

There is another linear coupling term, which couples \mathbf{A} with pair current $i(\eta_i^x \eta_j^y - \eta_i^y \eta_j^x)$, but $ig_{\text{eff}}(a - a^\dagger) \sum_{\langle ij \rangle} \xi_{ij} (n_i - n_j)$ should be the relevant term in the regime where CDW fluctuations are enhanced by the coupling to the cavity.

Nonlinearity in the photon states

To demonstrate the nonlinearity in the photon spectrum, we have computed all of the eigenvalues for the cavity-coupled Hubbard chain of $L = 6$. In this section, we give more details on the energy spectrum. The energy eigenvalues are shown in Fig. 7 for the blue-detuned cavity and in Fig. 8 for the red-detuned cavity. In the blue-detuned case, due to the relatively larger Ω , the few-photon states are rather protected by an energy gap and the photon number $N_{ph} = \langle a^\dagger a \rangle$ of the excited states is relatively discrete, taking values around the integers. Interestingly, the first photon gap $0 \rightarrow 1$ seems less robust, due a photoemission-like process where mobile electronic excitations are formed upon the absorption of a photon.

On the other hand, for the red-detuned case, there is a clear gap between $N_{ph} = 1$ and $N_{ph} = 0$ states, since the energy of one photon is well below U . However, the two-photon state appears to strongly mix with the electronic excitations, leading to superpositions of different photon-number sectors. Strictly speaking, in the large coupling regime $g \sim 0.4$, the $1 \rightarrow 2$ photon gap is not completely well-defined because $U = 2\Omega$ indeed satisfies the resonance condition. This results in the dramatic change in the $1 \rightarrow 2$ curve in Fig. 9. After all, the one-photon engineering regime appears to be well-defined, and should be accessible from an adiabatic injection of photons into the cavity.

By picking up the lowest-lying states in each photon-number sector, we show the effective photon gap in Fig. 9. In practice, due to the mixing between different photon-number states, we have actually set a photon number threshold $N_{ph} = 0.5$ (1.5) for the one-photon (two-photons) state. This turns out to give reasonable results at least for not-too-large coupling g .

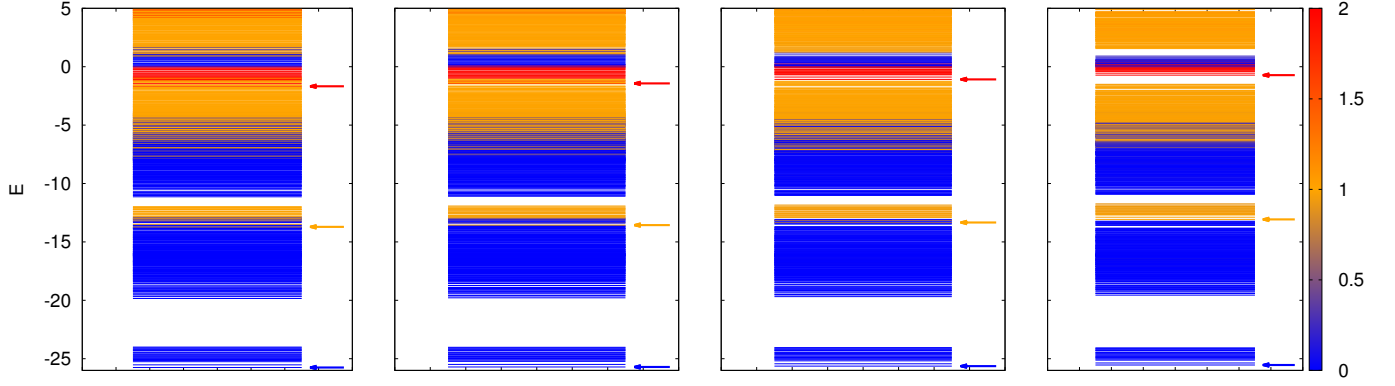


FIG. 7. The energy spectrum of $L = 6$ Hubbard chain coupled to the blue-detuned cavity ($\Omega = 1.5U$). The color represents the photon number N_{ph} . The arrows label the eigenstates picked up in the Fig. 9. The four panels correspond to $g = 0.1, 0.2, 0.3, 0.4$ from left to right, respectively.

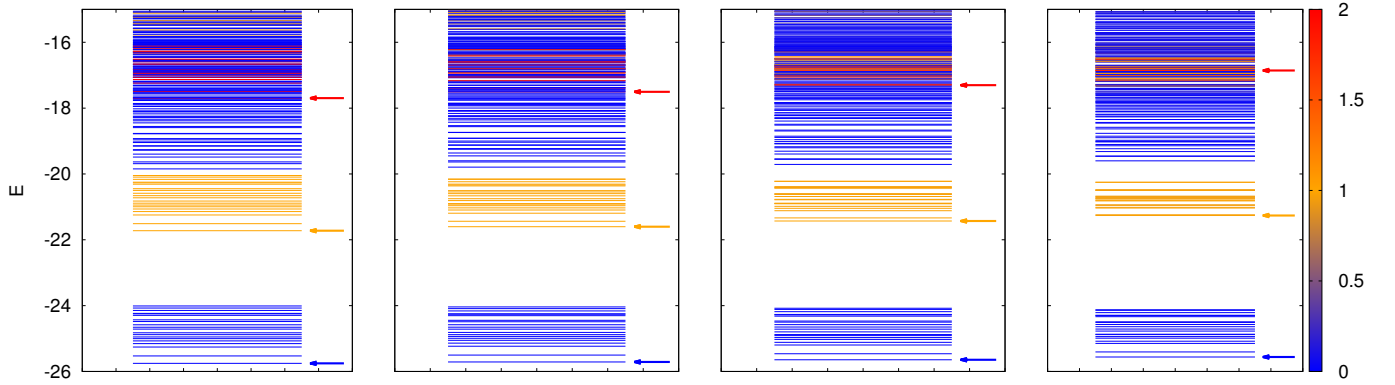


FIG. 8. The energy spectrum of $L = 6$ Hubbard chain coupled to the red-detuned cavity ($\Omega = 0.5U$). The color represents the photon number N_{ph} . The arrows label the eigenstates picked up in the Fig. 9. The four panels correspond to $g = 0.1, 0.2, 0.3, 0.4$ from left to right, respectively.

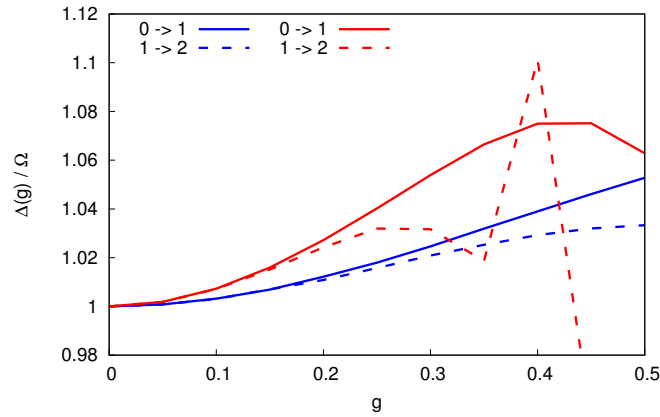


FIG. 9. The shift in photon energy gaps due to light-matter coupling. The energy gaps are obtained by picking up the lowest-lying eigenstates with photon-number $n = 0, 1, 2$ and evaluating the energy difference for an $L = 6$ cavity-Hubbard chain. The red (blue) curves correspond to $\Omega/U = 0.5$ ($\Omega/U = 1.5$). In the red-detuned regime, the $n = 2$ sector strongly mixes with electronic excitations, resulting in dramatic changes in the $1 \rightarrow 2$ curve for larger coupling.